Budd–Chiari Syndrome: Typical and Atypical Scintigraphic Aspects

Michel Picard, Lucie Carrier, Raymonde Chartrand, Pierre Franchebois, Daniel Picard, and Jean Guimond

Department of Nuclear Medicine and Department of Surgery, University of Montreal, Hôpital Saint-Luc, Québec, Canada

Budd–Chiari syndrome, a well known entity, is often difficult to diagnose, mostly due to the nonspecificity of its symptomatology. Radiocolloid liver scans were evaluated in eight cases of this disease, proven by surgical biopsy. Five cases showed the "classic" scintigraphic pattern of caudate lobe hypertrophy (62.5%), and other abnormalities observed included segmental hepatic insufficiency, diffuse hepatic insufficiency, and relative hypertrophy of both the caudate lobe and a portion of the parenchyma of segment VI (one case each). An experimental study of hepatic venous drainage performed on livers at autopsy revealed four groups of accessory hepatic veins in addition to the main hepatic veins. The occlusion of various parts of this drainage appears to relate to the various scintigraphic patterns that were encountered in patients with Budd–Chiari syndrome. A review of the literature revealed three additional patterns previously reported in association with Budd–Chiari syndrome (normal scan, diffuse hepatomegaly, and multiple filling defects). If all these variations are appreciated, liver scanning can be a valuable screening tool for Budd–Chiari syndrome and may also serve as a noninvasive means of follow-up.

J Nucl Med 28:803–809, 1987

Since its first description by Budd (1845) and Chiari (1899) (*1,2*), the diagnosis of hepatic venous occlusion has remained difficult. The low prevalence of the syndrome (<0.05% of autopsy findings) (*3*) is certainly a contributing factor but, more than likely, the major element is the nonspecificity of its symptomatology (*4,8*), which includes diffuse hepatomegaly (70%–100%), ascites (90%–95%), abdominal pain (55%), splenomegaly (30%–35%), and mild jaundice (30%).

Radiocolloid liver scan may facilitate the diagnosis of Budd–Chiari syndrome (*8*), but there is no pathognomonic scintigraphic pattern, and several more or less typical patterns may be encountered. In this paper, we review these patterns and their underlying pathophysiology.

MATERIALS AND METHODS

Among all suspected cases of Budd–Chiari syndrome occurring in our institution within the last 10 yr, we reviewed eight cases that were proven by surgical liver biopsies. Hepatic vein catheterization was successfully performed in six patients and actual demonstration of the distribution of thrombosis was obtained, allowing us to eventually correlate both thrombotic and scintigraphic findings in these patients.

In each case, the initial diagnostic tool was a liver scan; further investigations were done on the basis of liver scan abnormality. Two early cases were imaged on a rectilinear scanner. The remainder (six cases) were imaged on a LFOV camera equipped with a low-energy, all-purpose collimator, 20 min after injection of 5 mCi of either technetium-99m (^{99m}Tc) sulfur colloid or [^{99m}Tc]phytate. Anterior, posterior, right lateral, and right oblique anterior views were obtained. Segmental uptake of the radiocolloid was interpreted according to Healey and Schroy's hepatic segmentation (*9,10*), which is based on the intrahepatic distribution of the portal elements (Fig. 1).

Four scintigraphic patterns were encountered in relation with the Budd–Chiari syndrome. In an attempt to explain the occurrence of these patterns, as well as their respective underlying anatomic and physiologic components, we undertook a detailed study of normal hepatic venous drainage patterns.

We studied 30 fresh liver specimens obtained from autopsies performed on subjects known to be free of any significant hepatopathy. After exteriorization of the liver and its vessels, a systematic identification was carried out of both the main (right, middle, and left) and accessory hepatic veins. The

Received Feb. 13, 1986; revision accepted Oct. 1, 1986.

For reprints contact: Lucie Carrier, MD, Div. of Nuclear Medicine, Hôpital Saint-Luc, 1058 St-Denis, Montréal, Québec, Canada H2X 3J4.

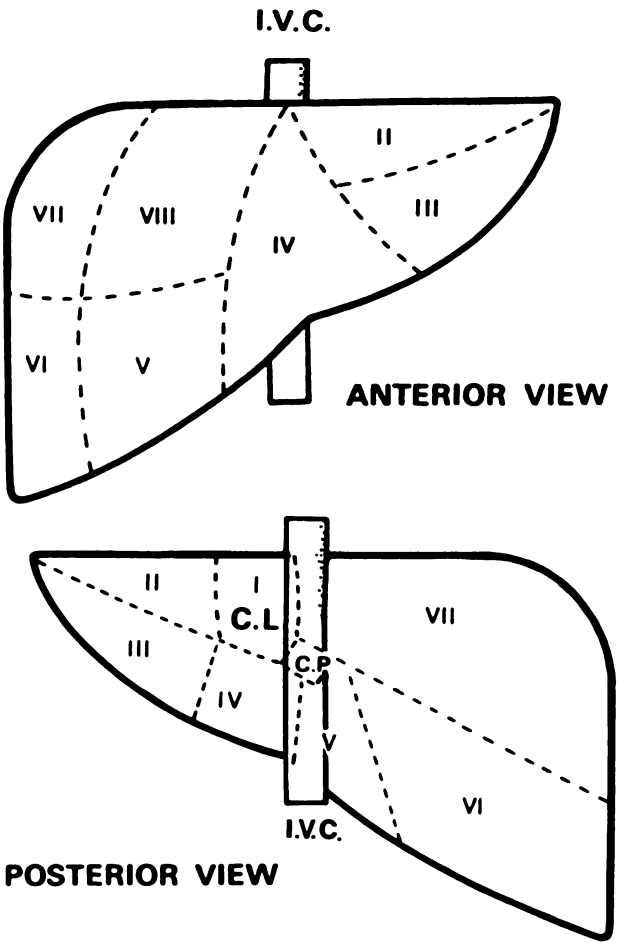

FIGURE 1
Hepatic segmentation according to Healey and Schroy (1953). Segment I: caudate lobe (C.L.) and caudate process (C.P.), II: supero-lateral segment, III: infero-lateral segment, IV: medial segment, V: antero-inferior segment, VI: postero-inferior segment, VII: postero-superior segment, VIII: antero-superior segment.

retrohepatic portion of the inferior vena cava was carefully exposed and a barium contrast medium was then injected into the ostium of each vein of 1 mm caliber or more. The portion of the hepatic parenchyma drained by each of these accessory hepatic veins, thus, was delineated. Each drainage area was then classified according to Healey and Schroy's hepatic segmentation.

RESULTS

In all eight cases, the surgical liver biopsies consistently showed hemorrhagic hepatocyte congestion and destruction, as well as slight perivascular fibrosis within the centrolobular areas. In four cases, the biopsies clearly showed thrombosis of branches of the main hepatic veins, establishing the diagnosis of Budd–Chiari syndrome.

Several scintigraphic patterns were encountered on radiocolloid liver scanning. Five cases (62.5%) showed caudate lobe hypertrophy, and we also observed one case each (12.5%) of segmental hepatic insufficiency, diffuse hepatic insufficiency, and relative hypertrophy of both the caudate lobe and a portion of the parenchyma of segment VI.

Caudate Lobe Hypertrophy

Of the five patients that demonstrated this pattern, three underwent hepatic vein catheterization and all demonstrated right, middle, and left hepatic vein thrombosis. Hepatic scintiscan showed a diffusely decreased radiocolloid uptake except for the caudate lobe, which showed relative hypertrophy and increased colloid uptake (Figs. 2 and 3). A slight hepatomegaly and

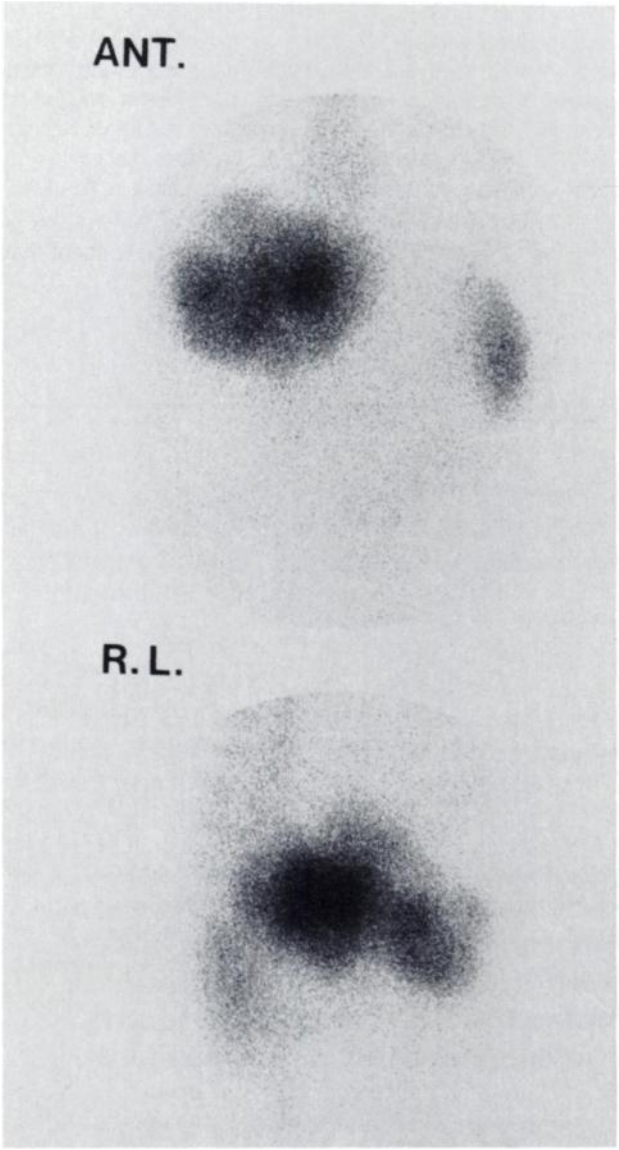

FIGURE 2
Budd–Chiari syndrome: typical scintigraphic pattern. Caudate lobe hypertrophy and significant medullary uptake of [^{99m}Tc]sulfur colloid.

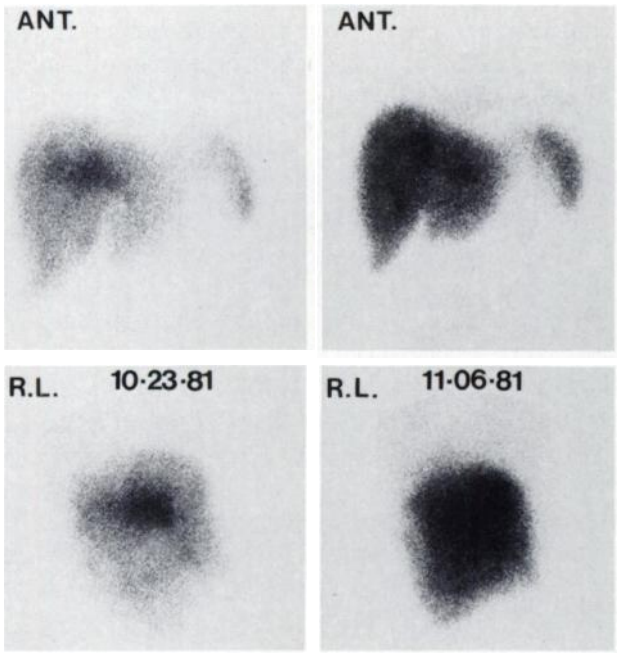

FIGURE 3
Budd–Chiari syndrome: typical scintigraphic pattern. On 10/23/1981, [^{99m}Tc]sulfur colloid hepatic uptake is diffusely decreased except for the caudate lobe, which is hypertrophic and relatively hyperfunctional. The patient had portocaval shunt and a follow-up scan was done on 11/06/1981, which was normal.

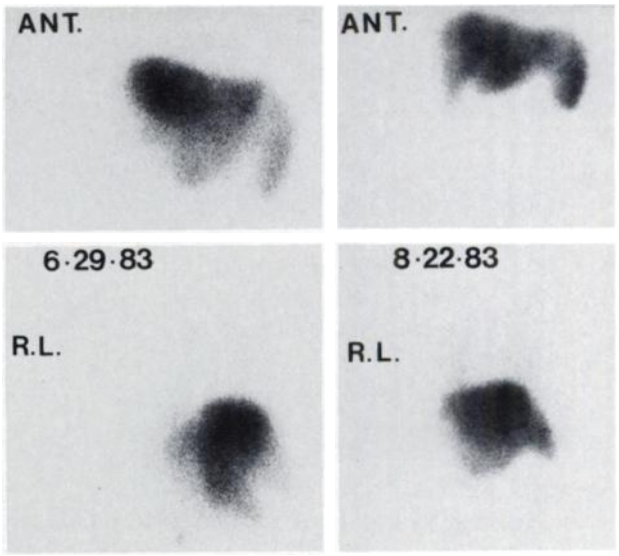

FIGURE 4
Budd–Chiari syndrome: segmental hepatic insufficiency. On 6/29/1983, liver scan shows no significant right lobe radiocolloid uptake due to complete right main hepatic vein occlusion. Normal left lobe concentration due to patency of the left main hepatic vein. Relative hypertrophy and increased uptake of the caudate lobe. Discrete bone marrow visualization. On 8/22/1983, following a successful portocaval shunt, right hepatic lobe appears much more functional. A slight caudate lobe hypertrophy persists.

splenomegaly can also be expected, as well as a discrete radiocolloid uptake within the medullary endothelial system. Following a successful latero-lateral portocaval shunt, the liver scan became completely normal (Fig. 3).

Segmental Hepatic Insufficiency

In the one patient showing this abnormality, hepatic vein catheterization showed complete right and partial left hepatic vein thrombosis and a patent middle hepatic vein. The initial liver scan (Fig. 4) showed a diffusely decreased colloid uptake within the right hepatic lobe, whereas, the left showed normal uptake; the caudate lobe showed a relative degree of hypertrophy, as well as increased colloid uptake. Discrete medullary uptake was also seen. Following a successful portocaval shunt, partial normalization of the liver scan occurred (Fig. 4).

Diffuse Hepatic Insufficiency

The hepatic vein catheterization in this patient showed inferior vena caval thrombosis in addition to right, middle, and left hepatic vein occlusion. This pattern consists in diffuse decreased liver colloid uptake with increased splenic and medullary uptake. There is no caudate lobe hypertrophy (Fig. 5). This pattern may be difficult to differentiate from severe cirrhosis. Fortunately, the clinical context is generally clear.

Relative Preservation of Function Within a Segment Other than the Caudate Lobe

In this patient, hepatic vein study showed right, middle, and left hepatic vein thrombosis with a patent inferior vena cava. The initial liver scan (Fig. 6) showed

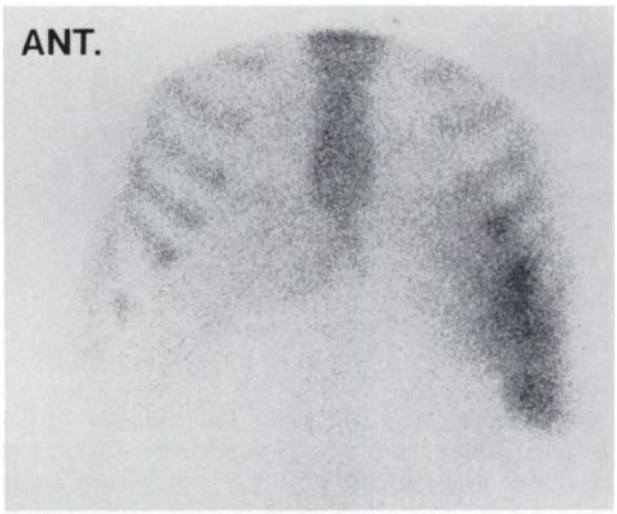

FIGURE 5
Budd–Chiari syndrome: diffuse hepatic insufficiency. Radiocolloid uptake decreased diffusely, due to complete hepatic venous occlusion without preservation of any collateral or accessory venous pathway. Radiocolloid redistribution towards spleen and marrow.

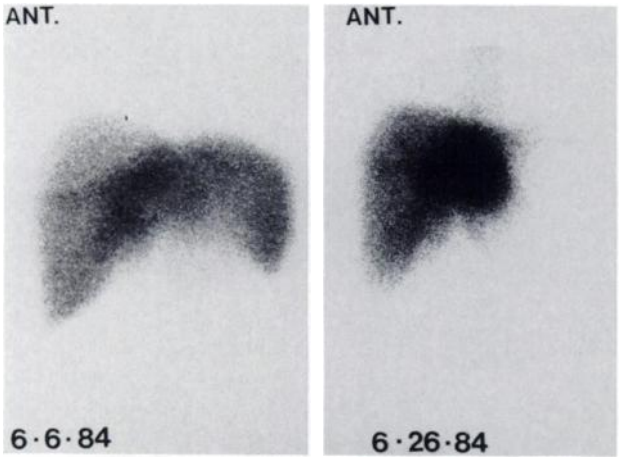

FIGURE 6
Budd–Chiari syndrome: functional preservation of a segment other than the caudate lobe. This atypical scintigraphic pattern consists of diffusely decreased hepatic [^{99m}Tc]sulfur colloid uptake, except in the segment VI vein region—i.e., segment VI and parts of segment V. Concomitant preservation of the caudate lobe is observed.

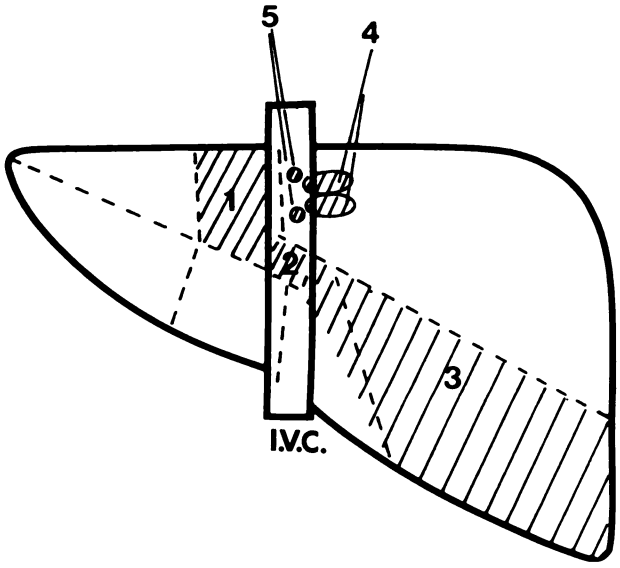

FIGURE 7
Posterior view of the liver and its accessory vein drainage areas. I.V.C.: inferior vena cava. Drainage territories of: (name, prevalence, dimension, mean number and drainage). 1. Segment I vein: 100%, 3 mm, 2, caudate lobe and process. 2. Caudate process vein: 23%, 1 mm, 1, caudate process. 3. Segment VI vein: 57%, 5 mm, 1, segment VI and portion of segment V. 4. Paracaval veins of segment VII: 80%, 2.5 mm, 1.7, (±3 cm) right posterior paracaval ellipse. 5. Precaval veins of segment VII: 67%, 1.3 mm, 1.9, small area posterior segment VII.

relatively diffuse and discrete reduction in colloid uptake, whereas, the caudate lobe showed discrete hypertrophy. Slightly increased uptake was also seen in the inferior segments of the right lobe, particularly within segments V and VI. A latero-lateral portocaval shunt was performed to alleviate sinusoidal pressure and restore hepatic venous flow. Spontaneous deterioration occurred 7 days postoperatively (Fig. 6).

Normal Hepatic Venous Drainage

The detailed study of liver specimens at autopsy showed that, apart from the main (right, middle, and left) hepatic vein, hepatic venous outflow also occurred through four main groups of accessory hepatic veins all located around the retrohepatic portion of the inferior vena cava (Fig. 7). Only the segment I veins encompassing the caudate process and the segment VI veins located on the right inferior margin of the retrohepatic portion of the inferior vena cava drains a large enough area to be scintigraphically significant. Segment VII vein drainage rarely exceeds a few centimeters in diameter and, thus, are of little clinical relevance.

DISCUSSION

Budd–Chiari syndrome is a relatively rare entity, involving symptomatic hepatic venous occlusion. Its etiology may often remain elusive. However, the literature published between 1960 and 1980 shows that underlying disorders can now be detected in 70% of patients. In Western countries, hematologic disorders and particularly polycythemia rubra vera predominate, whereas, in Japan and the Orient, the most frequently encountered disorder is a membranous web in the inferior vena cava (*7*).

Whatever the underlying cause of the Budd–Chiari syndrome, however, the pathophysiology involved is somewhat similar. Symptomatic hepatic venous occlusion may arise either from thrombosis (Budd–Chiari), external compression (pseudo Budd–Chiari) (*7*), or an abnormal endothelial proliferation (hepatic venoocclusive disease); once occlusion has occurred, the subsequent events are quite predictable and virtually consistent (*3,6,12,17*).

Following hepatic venous occlusion, centrolobular vein congestion and sinusoidal congestion supervene, accounting for the subsequent secondary reduction of hepatic afferent arterial flow and relative hepatic ischemia with atrophy and pressure necrosis of hepatocytes and centrolobular stroma (*5*). Venous outflow then generally proceeds through unusual venous pathways (*20*), via intrahepatic collateral veins from adjacent hepatic segments (in the case of incomplete Budd–Chiari), through subcapsular collateral veins or even by backflow within the portal vein.

Depending upon the particular venous drainage pathways that remain patent, it can be conceived that the physiologic and scintigraphic sequelae may vary considerably.

A review of the literature reveals that the clinical

presentation of Budd–Chiari syndrome does indeed vary (*4,8*) and several scintigraphic patterns (*3–35*) have been encountered on colloid liver scans in the 131 patients reported. Seven different scintigraphic patterns have been described in association with proven Budd–Chiari cases (Table 1). Although three of these cases (normal liver scan, diffuse hepatomegaly, and multiple filling defects) are not primarily suggestive of Budd–Chiari syndrome, we believe that clinicians should be more alert to the possibility of Budd–Chiari syndrome on observing the four patterns described in the patients included in this report (caudate lobe hypertrophy, segmental hepatic insufficiency, diffuse hepatic insufficiency, and functional preservation of a segment other than the caudate lobe).

A normal liver scan was reported in four cases (32%) of those reported by Khuroo et al. (*25*) and, although the diagnosis of Budd–Chiari syndrome was proven by liver biopsy, no detailed discussion of the underlying hepatic venous drainage pathways was offered.

Diffuse hepatomegaly with or without nonhomogeneous colloid uptake occurred in 19.8% of cases reported in the literature (26 of 131) (*7,13,25,28,30*). Although this pattern is relatively frequent it is, unfortunately, nonspecific and the differential diagnosis would rather be oriented towards steatosis, hepatitis, or cirrhosis of the liver. A high degree of clinical alertness is necessary, thus, and final diagnosis may depend on liver biopsy.

Liver scans showing multiple filling defects suggestive of space-occupying lesions occurred in 6.1% of cases (8 of 131) (*8,22,25,28,34*). Although most of these were reported in patients known to have some preexisting hepatopathy, at least one case occurred in the absence of any underlying unrelated liver disease (*22*). This pattern, unfortunately, is nonspecific because multiple filling defects may be associated with abscesses, cysts, primary tumor of the liver, pseudotumors of cirrhosis, or even regenerating nodules (*22*). Nevertheless, it should be kept in mind as possibly suggestive of Budd–Chiari syndrome, especially when clinical context renders the above mentioned diagnosis unlikely. In each case, more definitive studies such as hepatic angiography and hepatic venography may prove necessary. This scintigraphic pattern generally is attributed to the existence of intrahepatic shunting, liver deformity, and local impairment of Kupffer cell function (*34*). It occurs in cases of incomplete hepatic vein occlusion as proven in at least one case (*8*), and reflects the existence of interspersed areas of hepatic necrosis and hypertrophy, which are dependent on local venous perfusion pathways.

TABLE 1
Scintigraphic Patterns Associated with Budd–Chiari Syndrome in 131 Previously Reported Cases

Liver scan function	Number of cases	Cases (%)
Caudate lobe hypertrophy	83	63.4
Diffuse hepatomegaly	26	19.8
homogenous	(5)	(3.8)
nonhomogenous	(21)	(16.0)
Segmental hepatic insufficiency	8	6.1
right lobe	(6)	(4.6)
left lobe	(2)	(1.5)
Diffuse hepatic insufficiency	1	0.8
Space occupying lesion	8	6.1
Normal scan	4	3.0
Isolated function in segment other than caudate lobe	1	0.8

In caudate lobe hypertrophy, the liver scan demonstrates diffusely decreased radiocolloid uptake, except for the caudate lobe, which shows relative hypertrophy and increased colloid uptake. This occurred in five of our eight cases (62.5%). It is also the pattern most frequently reported in the literature (63.3%), and it can reasonably be considered typical of Budd–Chiari syndrome. Pathophysiologically, it generally results from complete main hepatic vein occlusion with persistent patency of the caudate lobe (segment I) vein (*24,25,30*), which drains directly within the retrohepatic portion of the inferior vena cava. In an experimental study we conducted on liver specimens taken at autopsy, the caudate lobe vein is a constant feature and can be found in all specimens (100%). Furthermore, its mean diameter (3 mm) is sufficient to provide effective hepatic venous drainage, provided the inferior vena cava is not also occluded.

The pattern of segmental hepatic insufficiency consists in relatively homogeneous decreased uptake within a well-circumscribed hepatic segment or lobe. To date, six cases (4.6%) of right hepatic lobe insufficiency (*4,5,29*) and two cases (1.5%) of left lobe insufficiency (*4,7*) have been reported, for a total of 6.1%. One of our eight cases (12.5%) showed right hepatic lobe insufficiency. This higher incidence is most certainly artefactual, due to the limited size of the population studied by us. Nevertheless, this relatively infrequent pattern is highly suggestive of Budd–Chiari syndrome because few other diseases cause complete hepatic insufficiency that is segmental in nature. The possibility of partial hepatectomy, radiation injury, fortuitous segmental involvement by focal or diffuse liver disease, and hepatic artery occlusion (*29*) must still be kept in mind, but such occurrences are either very rare or generally found in a clear clinical context.

Diffusely decreased colloid uptake with massive redistribution towards the spleen and the medullary endothelial system is rarely encountered (0.8%) (*28*). When fulminant hepatitis or terminal cirrhosis of the liver are clinically unlikely, this extremely rare pattern should nevertheless suggest the possibility of Budd–Chiari syn-

drome. As we were able to demonstrate with hepatic venography and cavography (Case 7), this pattern results from complete main hepatic vein occlusion with concomitant occlusion of the inferior vena cava preventing the caudate lobe vein from playing its beneficial role. Effective venous drainage through any of the accessory hepatic veins is then impossible. The situation is particularly critical and death must be considered imminent.

Whenever a major occlusion of the main hepatic veins occurs, and because the caudate lobe vein is constantly present, liver scintiscan usually shows caudate lobe hypertrophy. Our experimental study of liver specimens from autopsies, however, demonstrate that several other accessory hepatic veins usually exist. In fact, most specimens studied had five accessory hepatic veins of more than 1 mm in caliber. Unfortunately, only segment VI veins drain an area sufficiently extensive to be seen scintigraphically. In fact, segment VI veins are often bigger (5 mm diameter) than their caudate lobe counterpart (3 mm diameter) but they are not always present (57% of our autopsy cases) unlike the caudate lobe vein.

Segment VI veins drain not only the latero-inferior portion of the right hepatic lobe (segment VI) but also the more central and superior aspect of segment V. One of our cases actually showed relative caudate lobe hypertrophy, as well as relative functional preservation of some of segment V and VI parenchyma (Fig. 6). Such a pattern has not been reported yet in the literature. However, in a recent case report, Simon and Olsen (*35*), while mentioning the possible occurrence on liver scan of a pattern consistent with hepatic regenerative nodules, possibly overlooked the fact that a definite increased colloid uptake was initially present in the infero-lateral margin of the right hepatic lobe (segment VI). We believe that this case is another example of the clinical evidence of preserved patency of the segment VI vein.

Rossleigh et al. (*8*) reported an unusual case of markedly increased radionuclide accumulation at the inferior junction of the right and left hepatic lobes, which they attributed to abnormal collateral flow through the umbilical vein. From this case report and from our experimental studies, it would appear plausible that several other scintigraphic patterns may yet be possible. Nevertheless, caudate lobe hypertrophy remains the most frequently encountered pattern and may be considered typical of Budd–Chiari syndrome. As previously discussed, more atypical scintigraphic aspects must also alert the clinician to the possibility of such a diagnosis.

Liver colloid scan is a good screening test (*8*) for Budd–Chiari syndrome that may also prove to be a noninvasive follow-up technique (*16*) and a useful means of assessing therapeutic maneuvers as we have demonstrated for three of our patients (two of whom improved, the other deteriorating following portocaval shunt). Furthermore, a knowledge of the patency of certain accessory venous drainage pathways within the inferior vena cava ultimately may be of interest to the surgeon who has to decide on the timing and nature of the surgical approach to be employed.

ACKNOWLEDGMENTS

The authors thank Liette Babin of St-Luc Hospital for the technical assistance provided and the Photography Departments of Hôtel-Dieu de Montréal Hospital and St-Luc Hospital for the illustrations.

REFERENCES

1. Budd G. On disease of the liver, 1st ed. London: J and A Churchill Ltd, 1849:146.
2. Kiari H. Ueber der selbstandige phlebitis obliterans der hanptamme der venae hepaticae als todesursache. *Beitr Path Anat* 1899; 26:1.
3. Bockus HL. Hepatic vein thrombosis (Budd–Chiari syndrome). In: Gastroenterology. Philadelphia: W.B. Saunders, 1976:484–486.
4. Clain D, Freston J, Sherlock S. Clinical diagnosis of the Budd–Chiari Syndrome. *Am J Med* 1967; 43:544, 554.
5. Staab EV, Hartman RC, Parrott JA. Liver imaging in the diagnosis of hepatic venous thrombosis in paroxysmal nocturnal hemoglobinuria. *Radiology* 1975; 117:341–348.
6. Sherlock S. Diseases of the liver and biliary system, 6th ed. London: Blackwell Scientific Publications, 1981:180–186.
7. Mitchell MC, Boitnott JK, Kaufman S, et al. Budd–Chiari syndrome: etiology, diagnosis and management. *Medicine* 1982; 61:199–218.
8. Rossleigh MA, Uren RF, Morris JG. Radionuclide liver scan: a screening test for the Budd–Chiari syndrome. *Med J Austral* 1984; 140:234–236.
9. Healey JE, Schroy PC. Anatomy of the biliary ducts within the human liver. *Arch Surg* 1953; 66:599–616.
10. Healey JE, Schroy PC, Sorensen RJ. The intrahepatic distribution of the hepatic artery in man. *J Int C Surg* 1953; 20:133–148.
11. Floyd JL. The radiographic gamut of Budd–Chiari syndrome. *Am J Gastr* 1981; 76:381–387.
12. Galloway S, Casarella WJ, Price JB. Unilobar venoocclusive disease of the liver. *Am J Roentgenol Radium Ther* 1973; 119:89–94.
13. Baert AL, Fevery J, Marchal G, et al. Early diagnosis of Budd–Chiari syndrome by computed tomography and ultrasonography: report of five cases. *Gastroenterology* 1983; 84:587–595.
14. Simon DC, Olsen JO. The development of regenerative nodules in Budd–Chiari syndrome demonstrated by liver scan. *Clin Nucl Med* 1985; 10:374–375.
15. Parker RGF. Occlusion of the hepatic veins in man. *Medicine* 1959; 38:369.
16. Lisbona R, Katz S, Mishkin S. Serial radionuclide liver imaging in Budd–Chiari syndrome. *J Canad Assoc Radiol* 1981; 32:175–177.
17. Dhawan VM, Sziklas JJ, Spencer RP. Pseudo-Budd–

Chiari syndrome. *Clin Nucl Med* 1978; 3:30–31.
18. Fajardo LF, Colby TV. Pathogenesis of veno-occlusive liver disease after radiation. *Arch Pathol Lab Med* 1980; 104:584–588.
19. Reynolds TB, Peters RL. In: Schill L, Schiff ER, eds. Budd–Chiari syndrome, diseases of the liver, 5th ed. J.B. Lippincott Co, 1982:1622–1630.
20. Pollard JJ, Nebesar RA. Altered hemodynamics in the Budd–Chiari syndrome demonstrated by selective hepatic and selective splenic angiography. *Radiology* 1967; 89:236–243.
21. Chaudhuri TK, Chaudhuri TK. Liver scan in the Budd–Chiari syndrome. *J Am Med Assoc* 1972; 221:506–507.
22. Singh A, Farrer PA. Filling defects in Budd–Chiari syndrome. *NY State J Med* 1980; 80:801–802.
23. White CL. Clinical conferences at the Johns Hopkins Hospital clinical-pathologic conference. *Johns Hopkins Med J* 1980; 147:41–46.
24. Tilialos M, et al. The Budd–Chiari syndrome in pregnancy. *Postgrad Med J* 1978; 54:686–691.
25. Khuroo MS, Datta DV. The hepatic scintigraphy in Budd–Chiari syndrome: diagnostic value and further observations on the pathogenesis of the abnormal findings. *J Assoc Physicians India* 1979; 27:795–802.
26. Carulli N, Boraldi F, Roncaia R, et al. Liver scan in the Budd–Chiari syndrome. *J Am Med Assoc* 1973; 223:1161.
27. Thijs LG, Heidendal GAK, Huijens PC, et al. The use of nuclear medicine procedures in the diagnosis of Budd–Chiari syndrome. *Clin Nucl Med* 1978; 3:389–392.
28. Caroli J, Guille C. Diagnostic scintigraphique et artériographique du syndrome de Budd–Chiari. *Revue Médico-Chir Mal Foie* 1971; 46:211–215.
29. Meindok H, Langer B. Liver scan in Budd–Chiari syndrome. *J Nucl Med* 1976; 17:365–368.
30. Tavill AS, Wood EJ, Kreel L, et al. The Budd–Chiari syndrome: correlation between hepatic scintigraphy and the clinical, radiological, and pathological findings in nineteen cases of hepatic venous outflow obstruction. *Gastroenterology* 1975; 68:509–518.
31. Uflacker R, Francisconi C, Rodriguez MP, et al. Percutaneous transluminal angioplasty of the hepatic veins for treatment of Budd–Chiari syndrome. *Radiology* 1984; 153:641–642.
32. Yang PJ, Glazer GM, Bowerman RA. Budd–Chiari syndrome: computed tomographic and ultrasonographic findings. *J Comput Assist Tomogr* 1983; 7:148–150.
33. Gasty I, Horovitz I, Keyvan A. The use of gallium-67 liver imaging for the early diagnosis of Budd–Chiari syndrome. *J Nucl Med* 1984; 25:320–322.
34. Hungerford GD, Hamlynan AP, Lunzer MR, et al. Pseudo-metastases in the liver: a presentation of the Budd–Chiari syndrome. *Radiology* 1976; 120:627–628.
35. Simon DC, Olsen JO. The development of regenerative nodules in Budd–Chiari syndrome demonstrated by liver scan. *Clin Nucl Med* 1985; 10:374–375.